2022 30th Mediterranean Conference on Control and Automation (MED)
June 28 - July 1, 2022. Athens, Greece

On the Design of Coordinated Impedance Control Laws for De-orbiting and De-Spinning of Cooperative Satellites*

Kostas Nanos and Evangelos Papadopoulos, *Fellow, IEEE*

Abstract. **In several on-orbit applications, such as de-orbiting, continuous contact between a servicing robot (chaser) and a serviced satellite (target) is needed. The task includes chaser free-space motion and subsequent contact interaction with a floating target. To achieve this, usually grasping of the satellite is proposed. However, most of the existing satellites on orbit have no dedicated grapple fixtures. In this paper, a coordinated impedance control law is proposed for the de-orbiting of a target via continuous contact and without grasping between the chaser end-effector and the target. Since both the manipulator's end-effector and the spacecraft base are controlled, the developed controller guarantees singularity avoidance in addition to maintaining continuous contact between the two bodies. Also, this controller is adapted to be employed in the de-spinning of a rotating satellite with known angular velocity via continuous contact. The developed control laws apply to spatial systems and are illustrated by planar examples.**

I. Introduction

On-orbit servicing is becoming a very important issue due to the rapid increase in the number of aging satellites and of space debris. Capture and deorbiting of space debris is an already pressing challenge, as their collision with operational satellites or structures in the same orbit can cause significant damage. To address this problem, space robotic systems can be employed. On-orbit servicing applications, such as capture, de-spinning, and de-orbiting, require continuous contact between a servicing manipulator (chaser) and a serviced satellite (target), see Fig. 1.

During a de-orbiting task, the chaser approaches the target satellite, which is floating freely in space, and following contact, directs the target for re-entry. As both the chaser and the target lack fixed bases, this task is very challenging. An important question that arises is whether a control strategy exists that will ensure that the two bodies will remain in contact throughout the task; if contact is lost, the target will move in an uncontrolled way, and de-orbiting may fail. Moreover, in impacts where high stiffness is involved, the target satellite may bounce away before the chaser has time to react, due to intrinsic time delays. In addition, many targets are spinning due to small residual angular momentum, increasing the difficulty of capture. A target can be detumbled by applying appropriate external torques on it [1]. These tasks also require continuous contact between the chaser and the target; else the target may drift from its desired trajectory. Therefore, the interaction of a robotic manipulator with its environment is important in both target de-orbiting and de-spinning.

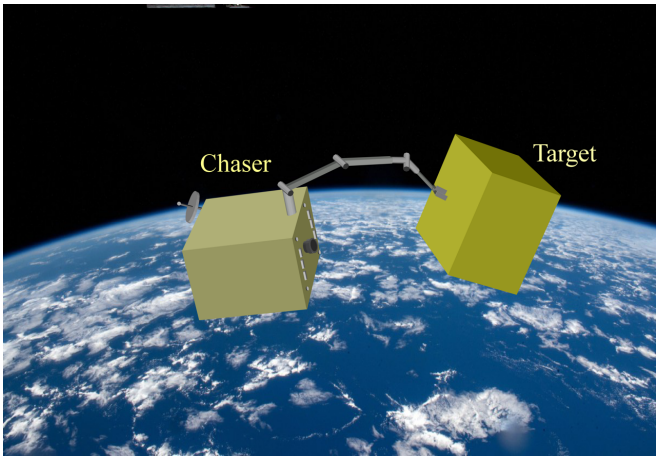

Fig. 1. A satellite (target) deorbiting by a robotic chaser.

To obtain a desired response and limit contact oscillations, an appropriate control method must be used. Impedance controllers are natural candidates for such interactions, [1] – [5]. A de-tumbling strategy by defining a desired target decelerating force/torque and scaled according to force/torque limits has been proposed in [6]. To capture rapid tumbling targets, a general friction contact model for complex contact geometries was developed [7]. To attenuate target rotation, a detumbling multipoint contact strategy was proposed in [8]. Considering target's parameter uncertainty, Wang et al., designed an integrated control framework including detumbling strategy and target's parameter identification [9]. A hybrid motion/force controller was developed to acquire desired contact forces and space robot configuration despite the floating nature of the system in [10]. However, all these works assume presence of a grapple fixture on the target.

The problem of continuous contact between two bodies lacking a rigid grasp and fixed bases has been studied in [11]. It was shown that continuous contact can be achieved by setting an appropriate chaser velocity at contact, accompanied by an impedance controller. The same controller was applied in both phases without switching, avoiding loss of contact, and instabilities due to unavoidable transition delays and unknown properties. However, although both thrusters and reaction wheels were used, the position/ attitude of the space-

* Kostas Nanos' research is co-financed by Greece and the European Union (European Social Fund-ESF) through the Operational Programme «Human Resources Development, Education and Lifelong Learning» in the context of the project "Reinforcement of Postdoctoral Researchers - 2nd Cycle" (MIS-5033021), implemented by the State Scholarships Foundation (IKY).
Kostas Nanos and Evangelos Papadopoulos are with the School of Mechanical Engineering, National Technical University of Athens, Athens, Greece (phone: +30-210-772-1440; fax: +30-210-772-1450; e-mail: nanos.kostas@gmail.com, egpapado@central.ntua.gr).

craft (S/C) were not controlled; eventually leading to singularities (i.e., manipulator outstretched) and contact loss.

In this paper, a coordinated impedance control law is proposed for the de-orbiting of a target via continuous contact and without grasping between the chaser end-effector and the target. Since both the manipulator's end-effector and the spacecraft base are controlled, the developed controller guarantees singularity avoidance, in addition to maintaining continuous contact between the two bodies. Next, this control law is modified to be applicable to de-spinning operations, where the elimination of target rotation of known angular velocity is desired. The developed control laws apply to spatial systems and are illustrated by planar examples.

II. System Dynamics

A. Target Dynamics

The target is floating freely in space. It is assumed that its motion state (e.g., angular velocity) and the mass properties (e.g., center of mass (CoM) position) of the target are known. During the contact phase, an external force $\mathbf{f}_{ext}$ and a moment $\mathbf{n}_{ext}$ with respect to the free-floating object (target) CoM act on it. The target equations of motion are

$$\mathbf{f}_{ext} = m_t \ddot{\mathbf{r}}_t \tag{1}$$

and

$$\mathbf{n}_{ext} = \mathbf{r}_0^{\times}\, \mathbf{f}_{ext} = \mathbf{I}_t \dot{\boldsymbol{\omega}}_t + \boldsymbol{\omega}_t^{\times}(\mathbf{I}_t \boldsymbol{\omega}_t) \tag{2}$$

where $(\cdot)^{\times}$ denotes the cross product matrix of vector $(\cdot)$, m_t and $\mathbf{I}_t$ is the target mass and moment of inertia matrix, respectively, $\mathbf{r}_0$ is the distance from the target CoM to the contact point, and $\boldsymbol{\omega}_t$, and $\mathbf{r}_t$ are the target angular velocity, and the position vector of its CoM with respect to the inertial frame, respectively.

B. Chaser Dynamics

An on-orbit space manipulator system (chaser) consists of a manipulator mounted on a S/C equipped with thrusters and momentum control devices, applying forces and moments on it. According to current practice in space, the chaser's manipulator has revolute joints and an open chain kinematic configuration, so that, in a system with an N degree-of-freedom (DoF) manipulator, there are $N+6$ DoFs in total. The chaser operates in *free-flying mode* when the S/C control system is active. In this case, the equation of motion of the chaser is given by, [11]

$$\mathbf{H}(\boldsymbol{\delta}_0, \mathbf{q})\ddot{\mathbf{z}} + \mathbf{c}(\boldsymbol{\delta}_0, \mathbf{q}, \dot{\boldsymbol{\delta}}_0, \dot{\mathbf{q}}) = \mathbf{Q}_{act} - \mathbf{Q}_{ext} \tag{3}$$

where $\mathbf{c}$ is the vector of the nonlinear Coriolis and centrifugal terms and,

$$\mathbf{z} = \begin{bmatrix} \mathbf{r}_{C_0}{}^T & \boldsymbol{\delta}_0{}^T & \mathbf{q}^T \end{bmatrix}^T \tag{4}$$

where $\mathbf{r}_{C_0}$ is the position vector of the chaser's S/C CoM with respect to an inertial frame, $\boldsymbol{\delta}_0$ is the column vector of a set of Euler angles describing the S/C attitude, and $\mathbf{q}$ is the column vector of the manipulator joint angles.

The $(6+N)\times(6+N)$ matrix $\mathbf{H}(\mathbf{q}, \boldsymbol{\delta}_0)$ is given by

$$\mathbf{H}(\boldsymbol{\delta}_0, \mathbf{q}) = \tilde{\mathbf{E}}^T(\boldsymbol{\delta}_0)\, \tilde{\mathbf{H}}(\mathbf{q})\, \tilde{\mathbf{E}}(\boldsymbol{\delta}_0) \tag{5}$$

where $\tilde{\mathbf{H}}(\mathbf{q})$ is the system inertia matrix, and

$$\tilde{\mathbf{E}}(\boldsymbol{\delta}_0) = \begin{bmatrix} \mathbf{I}_{3\times3} & \mathbf{0}_{3\times3} & \mathbf{0}_{3\times N} \\ \mathbf{0}_{3\times3} & \mathbf{E}(\boldsymbol{\delta}_0) & \mathbf{0}_{3\times N} \\ \mathbf{0}_{N\times3} & \mathbf{0}_{N\times3} & \mathbf{I}_{N\times N} \end{bmatrix} \tag{6}$$

where $\mathbf{I}_{k\times k}$ is the $k\times k$ unity matrix, $\mathbf{0}_{m\times n}$ is the $m\times n$ zero matrix, and $\mathbf{E}(\boldsymbol{\delta}_0)$ is a 3×3 matrix which relates the S/C angular velocity $\boldsymbol{\omega}_0$ to the Euler rates $\dot{\boldsymbol{\delta}}_0$.

The generalized forces $\mathbf{Q}_{act}$ are functions of the actuator forces $\mathbf{f}_s$ and moments $\mathbf{n}_s$ applied to the S/C CoM, and torques $\boldsymbol{\tau}$ applied to the joints. The generalized forces $\mathbf{Q}_{ext}$ are functions of the external forces $\mathbf{f}_{ext}$ and moments $\mathbf{n}_{ext}$ applied on the end-effector. The $\mathbf{Q}_{ext}$, $\mathbf{Q}_{act}$ are given by,

$$\mathbf{Q}_{ext} = \mathbf{J}_v^T \begin{bmatrix} \mathbf{f}_{ext} \\ \mathbf{n}_{ext} \end{bmatrix} = \mathbf{J}_v^T \boldsymbol{F}_{ext} \tag{7}$$

where $\mathbf{J}_v$ is a Jacobian matrix and

$$\mathbf{Q}_{act} = \begin{bmatrix} \mathbf{0}_{6\times1} \\ \boldsymbol{\tau} \end{bmatrix} + \mathbf{J}_s^T \begin{bmatrix} \mathbf{f}_s \\ \mathbf{n}_s \end{bmatrix} = \mathbf{J}_q \begin{bmatrix} \mathbf{f}_s^T & \mathbf{n}_s^T & \boldsymbol{\tau}^T \end{bmatrix}^T \tag{8}$$

where the Jacobian matrix $\mathbf{J}_s$ is,

$$\mathbf{J}_s = \begin{bmatrix} \mathbf{I}_{3\times3} & \mathbf{0}_{3\times3} & \mathbf{0}_{3\times N} \\ \mathbf{0}_{3\times3} & \mathbf{E}(\boldsymbol{\delta}_0) & \mathbf{0}_{3\times N} \end{bmatrix} \tag{9}$$

and the matrix $\mathbf{J}_q$ is given by,

$$\mathbf{J}_q = \begin{bmatrix} \mathbf{I}_{3\times3} & \mathbf{0}_{3\times3} & \mathbf{0}_{3\times N} \\ \mathbf{0}_{3\times3} & \mathbf{E}^T(\boldsymbol{\delta}_0) & \mathbf{0}_{3\times N} \\ \mathbf{0}_{N\times3} & \mathbf{0}_{N\times3} & \mathbf{I}_{N\times N} \end{bmatrix} \tag{10}$$

Since it is desired to control the pose (position/ orientation) of both the chaser's end-effector and S/C, the equations of motion of the chaser are written with respect to the S/C and end-effector pose.

The end-effector's velocity is given by

$$[\dot{\mathbf{r}}_e^T \quad \dot{\boldsymbol{\delta}}_e^T]^T = \mathbf{J}_e [\dot{\mathbf{r}}_{c_0}^T \quad \dot{\boldsymbol{\delta}}_0^T \quad \dot{\mathbf{q}}^T]^T = \mathbf{J}_e \dot{\mathbf{z}} \tag{11}$$

where $\mathbf{r}_e$ is the chaser's end-effector position with respect to the inertial frame, $\boldsymbol{\delta}_e$ is a set of Euler angles describing the end-effector's orientation and $\mathbf{J}_e$ is a Jacobian matrix.

The S/C velocity is given by

$$[\dot{\mathbf{r}}_{c_0}^T \quad \dot{\boldsymbol{\delta}}_0^T]^T = \mathbf{J}_r [\dot{\mathbf{r}}_{c_0}^T \quad \dot{\boldsymbol{\delta}}_0^T \quad \dot{\mathbf{q}}^T]^T = \mathbf{J}_r \dot{\mathbf{z}} \tag{12}$$

where $\mathbf{J}_r$ is a Jacobian matrix.

To set up the coordinated control law developed in this work, the system generalized speeds are defined as

$$\dot{\mathbf{x}} = [\dot{\mathbf{r}}_e^T \quad \dot{\boldsymbol{\delta}}_e^T \quad \dot{\mathbf{r}}_{c_0}^T \quad \dot{\boldsymbol{\delta}}_0^T]^T = \mathbf{J} [\dot{\mathbf{r}}_{c_0}^T \quad \dot{\boldsymbol{\delta}}_0^T \quad \dot{\mathbf{q}}^T]^T = \mathbf{J} \dot{\mathbf{z}} \tag{13}$$

where $\mathbf{J}$ is a Jacobian – type matrix given by,

$$\mathbf{J} = \begin{bmatrix} \mathbf{J}_e \\ \mathbf{J}_r \end{bmatrix} \tag{14}$$

Differentiating (13), the acceleration is obtained as

$$\ddot{\mathbf{x}} = \mathbf{J}\ddot{\mathbf{z}} + \dot{\mathbf{J}}\dot{\mathbf{z}} \tag{15}$$

Considering that the acceleration $\ddot{\mathbf{z}}$ is given by (3), the chaser's end-effector and S/C acceleration can be written as

$$\ddot{\mathbf{x}} = \mathbf{J}\mathbf{H}^{-1}(\mathbf{Q}_{act} - \mathbf{Q}_{ext} - \mathbf{c}) + \dot{\mathbf{J}}\dot{\mathbf{z}} \tag{16}$$

Although, in space applications, first a de-spinning task is carried out, followed by a de-orbiting one, here the control for the de-orbiting task is presented first, since it is less complex than the one for de-spinning tasks.

III. De-orbiting Impedance Control

The concept is illustrated in Fig. 2. First, the chaser's end-

effector is driven from its initial position to the target, Fig. 2(a). The contact between the two bodies is modeled by a generalized spring of stiffness $\mathbf{K}_e$. The direction of the force is chosen such that it minimizes attitude disturbances. Fig. 2(b) shows the beginning of the contact when the interaction force/ moment $\boldsymbol{F}_{ext}$ is still zero. In Fig. 2(c), contact has been achieved and the developed $\boldsymbol{F}_{ext}$ causes target motion. Our interest is to develop an appropriate control algorithm, select its parameters, and study the initial conditions needed to keep the two bodies in contact throughout the process.

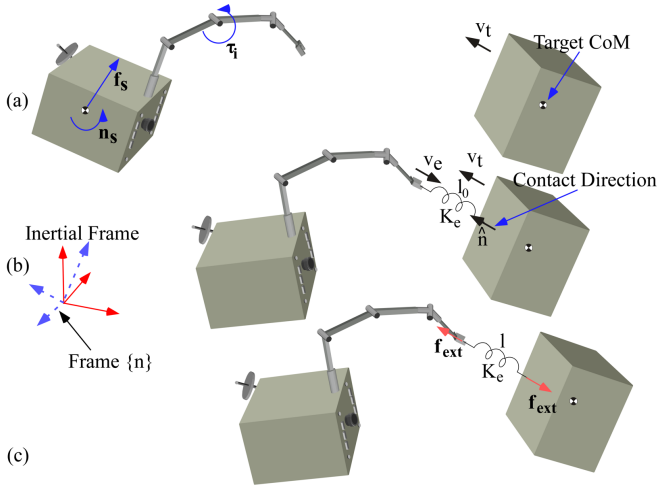

Fig. 2. (a) The chaser free motion, (b) the beginning of the contact and (c) the contact phase.

The controller sets an impedance behavior for both the end-effector and the S/C base. Additional important elements include the design of the desired applied forces on the target, and of the trajectories to achieve the task. To design the control law, the desired impedance performance for both the S/C and the end-effector are studied. Note that here, it is assumed that the target has been de-spined (see next section) and executes a translational motion only before the de-orbiting task.

A. Chaser's End-effector Desired Performance

Assuming point contact and negligible friction, only normal to the surface forces are developed, i.e., along the unit vector normal to the contact surface, $\hat{\mathbf{n}}$, see Fig. 2(b). The desired impedance behavior written in frame {n} whose origin coincides with the inertial frame's origin, and whose x-axis coincides with $\hat{\mathbf{n}}$, is [11],

$$\mathbf{M}_{d,e}\,{}^{n}\ddot{\mathbf{e}}_e+\mathbf{B}_{d,e}\,{}^{n}\dot{\mathbf{e}}_e+\mathbf{K}_{d,e}\,{}^{n}\mathbf{e}_e=-{}^{n}\boldsymbol{F}_{ext}+{}^{n}\boldsymbol{F}_{d,e} \tag{17}$$

where ${}^{n}(\cdot)$ denotes a vector/ matrix $(\cdot)$ expressed in frame {n}, and

$${}^{n}\boldsymbol{F}_{ext}={}^{n}\mathbf{K}_e\,{}^{n}\mathbf{e}_e \tag{18}$$

The vector $\mathbf{e}_e$ is the end-effector pose (i.e., position/ orientation) trajectory error defined as,

$$\mathbf{e}_e=\mathbf{x}_e-\mathbf{x}_{d,e}=[\mathbf{r}_e^T\quad\boldsymbol{\delta}_e^T]^T-[\mathbf{r}_{e,d}^T\quad\boldsymbol{\delta}_{e,d}^T]^T \tag{19}$$

where the variable $(\cdot)_d$ corresponds to the desired value of the variable $(\cdot)$.

The 6×6 impedance gain matrices $\mathbf{M}_{d,e}$, $\mathbf{B}_{d,e}$, $\mathbf{K}_{d,e}$ are,

$$\mathbf{M}_{d,e}=\mathrm{diag}(m_{d,e}),\mathbf{B}_{d,e}=\mathrm{diag}(b_{d,e}),\mathbf{K}_{d,e}=\mathrm{diag}(k_{d,e}) \tag{20}$$

It can be shown that the end-effector translational and attitude dynamics of the closed-loop system are governed according to the following impedance law written in inertial frame, [11]

$$\mathbf{M}_{d,e}\,\ddot{\mathbf{e}}_e+\mathbf{B}_{d,e}\,\dot{\mathbf{e}}_e+\mathbf{K}_{d,e}\,\mathbf{e}_e=-\boldsymbol{F}_{ext}+\boldsymbol{F}_{d,e} \tag{21}$$

where

$$\mathbf{e}_e=\mathbf{R}_n^*\,{}^{n}\mathbf{e}_e,\ \boldsymbol{F}_{ext}=\mathbf{R}_n^*\,{}^{n}\boldsymbol{F}_{ext},\ \boldsymbol{F}_{d,e}=\mathbf{R}_n^*\,{}^{n}\boldsymbol{F}_{d,e} \tag{22}$$

where $\mathbf{R}_n^*=\mathrm{diag}(\mathbf{R}_n,\mathbf{R}_n)$ and $\mathbf{R}_n$ is the rotation matrix between the inertial frame and frame {n}.

The desired force/ moment ${}^{n}\boldsymbol{F}_{d,e}$ is introduced to obtain non-zero steady state forces during contact. This force must be zero in the *free-space phase* for zero tracking error, while during the *contact phase* it must be non-zero, to ensure contact and non-zero steady state error. To avoid desired force switching, the desired force/ moment ${}^{n}\boldsymbol{F}_{d,e}$ is defined as,

$${}^{n}\boldsymbol{F}_{d,e}=\frac{\|\boldsymbol{F}_{ext}\|}{\|\boldsymbol{F}_{ext}\|+a}\,{}^{n}\boldsymbol{F}_{d,e}^{*} \tag{23}$$

where ${}^{n}\boldsymbol{F}_{d,e}^{*}$ is a non-zero constant column vector setting the desired contact force, and a is an arbitrary parameter of small value compared to $\|\boldsymbol{F}_{ext}\|$. During the free-space phase, the contact force/ moment $\boldsymbol{F}_{ext}$ is zero, and therefore ${}^{n}\boldsymbol{F}_{d,e}$ is also zero. However, during contact and for small a, ${}^{n}\boldsymbol{F}_{d,e}$ is about equal to the set value ${}^{n}\boldsymbol{F}_{d,e}^{*}$. The desired constant force/ moment in {n} is chosen as

$${}^{n}\boldsymbol{F}_{d,e}^{*}=[f_{d,e}^{*}\quad 0\quad 0\quad 0\quad 0\quad 0]^T \tag{24}$$

where $f_{d,e}^{*}$ is the desired force along contact direction $\hat{\mathbf{n}}$.

Also, to avoid controller switching, the desired trajectory $\mathbf{x}_{d,e}$ in (19) is defined as

$$\mathbf{x}_{d,e}(t)=\mathbf{x}_{d,e}^{f}(t)\frac{|1-\|\boldsymbol{F}_{ext}\|/a_1|}{1+a_1\|\boldsymbol{F}_{ext}\|}+\mathbf{x}_{d,e}^{c}(t)\frac{\|\boldsymbol{F}_{ext}\|}{\|\boldsymbol{F}_{ext}\|+a_2} \tag{25}$$

where $\mathbf{x}_{d,e}^{f}(t)$ and $\mathbf{x}_{d,e}^{c}(t)$ are the end-effector desired pose during the free space and contact phase, respectively, given in [11]. The parameters a_1 and a_2 are chosen large enough and small enough, respectively, so that $\mathbf{x}_{d,e}(t)=\mathbf{x}_{d,e}^{f}(t)$ in free-space, i.e. when $\|\boldsymbol{F}_{ext}\|=0$, and $\mathbf{x}_{d,e}(t)=\mathbf{x}_{d,e}^{c}(t)$ during the contact phase, i.e. when when $\|\boldsymbol{F}_{ext}\|\neq 0$.

The impedance gain matrices are selected considering a desired end-effector response either in the free space phase or in the contact phase. The requirement for the same controller (i.e., same controller gains) in both phases results in a dependence between the response in the contact phase (modeled as a spring of stiffness k_e), described by ζ_c and $\omega_{n,c}$, and the response in the free-space, given by ζ_f, and $\omega_{n,f}$, [11]

$$\zeta_c=\zeta_f\sqrt{k_{d,e}/(k_{d,e}+k_e)},\ \omega_{n,c}=\omega_{n,f}\sqrt{(k_{d,e}+k_e)/k_{d,e}} \tag{26}$$

Therefore, the selection of a desired critically damped (i.e., $\zeta_f=1$) or underdamped (i.e., $0<\zeta_f<1$) response in free space will result in an underdamped response during the contact phase. It has been shown that continuous contact of the chaser end-effector with the target is achieved if the initial relative velocity of the chaser end-effector along the contact direction with respect to the target is given by [11],

$$\mathbf{v}_\mathbf{d} = \mathbf{v}_\mathbf{e} - \mathbf{v}_\mathbf{t} = -(f^*_{d,e}\,\zeta_c / m_{d,e}\,\omega_{n,c})\,\hat{\mathbf{n}} \tag{27}$$

where $\mathbf{v}_\mathbf{e}$ is the chaser end-effector velocity at the beginning of the contact, and $\mathbf{v}_\mathbf{t}$ is the target velocity, see Fig. 2 (b).

The required end-effector velocity $\mathbf{v}_\mathbf{e} = \mathbf{v}_\mathbf{d} + \mathbf{v}_\mathbf{t}$ at the beginning of the contact phase is also the final end-effector velocity in the free-space phase and can be achieved by proper design of the desired trajectory $\mathbf{x}^\mathbf{f}_{\mathbf{d,e}}(t)$.

B. Chaser's S/C Desired Performance

The desired impedance performance for the chaser S/C is given by,

$$\mathbf{M}_{\mathbf{d,b}}\,\ddot{\mathbf{e}}_\mathbf{b} + \mathbf{B}_{\mathbf{d,b}}\,\dot{\mathbf{e}}_\mathbf{b} + \mathbf{K}_{\mathbf{d,b}}\,\mathbf{e}_\mathbf{b} = \mathbf{0}_{6\times1} \tag{28}$$

where $\mathbf{M}_{\mathbf{d,b}}$, $\mathbf{B}_{\mathbf{d,b}}$, $\mathbf{K}_{\mathbf{d,b}}$ are 6×6 impedance gain matrices,

$$\mathbf{M}_{\mathbf{d,b}} = \mathrm{diag}(m_{d,b}),\ \mathbf{B}_{\mathbf{d,b}} = \mathrm{diag}(b_{d,b}),\ \mathbf{K}_{\mathbf{d,b}} = \mathrm{diag}(k_{d,b}) \tag{29}$$

The error $\mathbf{e}_\mathbf{b}$ is defined as,

$$\mathbf{e}_\mathbf{b} = \mathbf{x}_\mathbf{b} - \mathbf{x}_{\mathbf{d,b}} = [\mathbf{r}^T_{c_0} \quad \boldsymbol{\delta}^T_\mathbf{0}]^T - [\mathbf{r}^T_{c_0,\mathbf{d}} \quad \boldsymbol{\delta}^T_{\mathbf{0,d}}]^T \tag{30}$$

where the desired S/C trajectory $\mathbf{x}_{\mathbf{d,b}}$ is defined as,

$$\mathbf{x}_{\mathbf{d,b}} = \mathbf{x}_\mathbf{e} - \mathbf{s}_\mathbf{0} \tag{31}$$

where the vector $\mathbf{s}_\mathbf{0}$ defines the desired distance between the end-effector and the S/C of the chaser expressed in the inertial frame.

The impedance gain matrices are selected such that (28) is stable. Then, the steady state error is zero, i.e., $\mathbf{e}_{\mathbf{b,ss}} = \mathbf{0}_{6\times1}$.

Considering (30)-(31), at steady state, the following holds,

$$\mathbf{x}_{\mathbf{e,ss}} - \mathbf{x}_{\mathbf{b,ss}} = \mathbf{s}_\mathbf{0} \tag{32}$$

C. Chaser's Total Desired Performance

Eqs. (21) and (28) can be written in a matrix form as

$$\mathbf{M}_\mathbf{d}\,\ddot{\mathbf{e}} + \mathbf{B}_\mathbf{d}\,\dot{\mathbf{e}} + \mathbf{K}_\mathbf{d}\,\mathbf{e} = -\bar{\boldsymbol{F}}_{\mathbf{ext}} + \bar{\boldsymbol{F}}_\mathbf{d} \tag{33}$$

where

$$\bar{\boldsymbol{F}}_{\mathbf{ext}} = [\boldsymbol{F}^T_{\mathbf{ext}} \quad \mathbf{0}^T_{6\times1}]^T \tag{34}$$

$$\mathbf{e} = [\mathbf{e}^T_\mathbf{e} \quad \mathbf{e}^T_\mathbf{b}]^T = [\mathbf{x}^T_\mathbf{e} \quad \mathbf{x}^T_\mathbf{b}]^T - [\mathbf{x}^T_{\mathbf{e,d}} \quad \mathbf{x}^T_{\mathbf{b,d}}]^T = \mathbf{x} - \mathbf{x}_\mathbf{d} \tag{35}$$

and the system impedance gain matrices are defined as,

$$\begin{aligned} \mathbf{M}_\mathbf{d} &= \begin{bmatrix} \mathbf{M}_{\mathbf{d,e}} & \mathbf{0}_{6\times6} \\ \mathbf{0}_{6\times6} & \mathbf{M}_{\mathbf{d,b}} \end{bmatrix},\ \mathbf{B}_\mathbf{d} = \begin{bmatrix} \mathbf{B}_{\mathbf{d,e}} & \mathbf{0}_{6\times6} \\ \mathbf{0}_{6\times6} & \mathbf{B}_{\mathbf{d,b}} \end{bmatrix} \\ \mathbf{K}_\mathbf{d} &= \begin{bmatrix} \mathbf{K}_{\mathbf{d,e}} & \mathbf{0}_{6\times6} \\ \mathbf{0}_{6\times6} & \mathbf{K}_{\mathbf{d,b}} \end{bmatrix},\ \bar{\boldsymbol{F}}_\mathbf{d} = \begin{bmatrix} \boldsymbol{F}_{\mathbf{d,e}} \\ \mathbf{0}_{6\times1} \end{bmatrix} \end{aligned} \tag{36}$$

D. Controller Design

Considering (33) - (35), the chaser end-effector and S/C acceleration is given by

$$\ddot{\mathbf{x}} = \mathbf{M}^{-1}_\mathbf{d}[-(\mathbf{B}_\mathbf{d}\,\dot{\mathbf{e}} + \mathbf{K}_\mathbf{d}\,\mathbf{e}) - \bar{\boldsymbol{F}}_{\mathbf{ext}} + \bar{\boldsymbol{F}}_\mathbf{d}] + \ddot{\mathbf{x}}_\mathbf{d} \tag{37}$$

The combination of (16) and (37) results in the following control law

$$\begin{aligned} &\mathbf{Q}_{\mathbf{act}} = \mathbf{Q}_{\mathbf{ext}} + \mathbf{c} \\ &+ (\mathbf{J}\mathbf{H}^{-1})^{-1}[\ddot{\mathbf{x}}_\mathbf{d} + \mathbf{M}^{-1}_\mathbf{d}(-\bar{\mathbf{f}}_{\mathbf{ext}} + \bar{\mathbf{f}}_\mathbf{d} - \mathbf{B}_\mathbf{d}\,\dot{\mathbf{e}} - \mathbf{K}_\mathbf{d}\,\mathbf{e}) - \dot{\mathbf{J}}\dot{\mathbf{z}}] \end{aligned} \tag{38}$$

where all the feedback variables can be measured by appropriate sensors.

Using (8), the actuator inputs are computed by

$$[\mathbf{f}^T_\mathbf{s} \quad \mathbf{n}^T_\mathbf{s} \quad \boldsymbol{\tau}^T]^T = \mathbf{J}^T_\mathbf{q}\,\mathbf{Q}_{\mathbf{act}} \tag{39}$$

IV. Target De-Spinning

In this section, the de-spinning of a spinning satellite of known angular velocity by contact, and despite the lack of a rigid grasp, is studied. Next, we focus on cases where the target is not tumbling but is initially spinning around an axis of fixed direction. During de-spinning, the chaser approaches the target satellite, which is rotating freely in space, and after contact, stabilizes the target's rotation by contact. The de-spinning task consists of the free space phase and the contact phase. Like in the de-orbiting task, in the free space phase the chaser's end-effector achieves the appropriate velocity required at the beginning of contact and the controller design is like the one developed in the de-orbiting operation. Here, we focus on the contact phase, see Fig. 3.

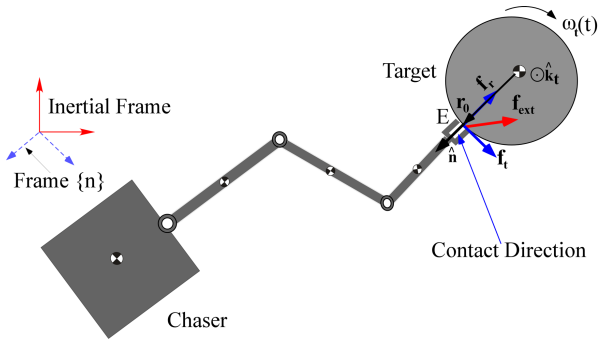

Fig. 3. The contact phase during de-spinning of the target by the chaser.

In the de-orbiting task, ${}^n\boldsymbol{F}_{\mathbf{d,e}}$ in (17) was a non-zero constant column vector setting the desired contact force. Next, a new form of ${}^n\boldsymbol{F}_{\mathbf{d,e}}$ for the de-spinning task is defined.

To stop target spinning without causing other undesirable rotations about other axes, the applied moment on the target $\mathbf{n}_{\mathbf{ext}}$ must have direction such that the target angular velocity $\boldsymbol{\omega}_\mathbf{t}(t)$, is reduced as specified, i.e.,

$$\mathbf{n}_{\mathbf{ext}} = \mathbf{r}^\times_\mathbf{0}\,\mathbf{f}_{\mathbf{ext}} = -k\,\boldsymbol{\omega}_\mathbf{t}(t),\ k>0 \tag{40}$$

In this case, the required desired applied external force is,

$$\mathbf{f}_{\mathbf{ext}} = \lambda\,\mathbf{r}_\mathbf{0} + (-k\,\boldsymbol{\omega}_\mathbf{t}(t))^\times\,\mathbf{r}_\mathbf{0}\,/r^2_0,\ \ \lambda\in R \tag{41}$$

where $r_0 = \|\mathbf{r}_\mathbf{0}\|$ and the coefficients k, λ are both limited by the system actuator capabilities. The first term is the *contact force* along the normal direction, i.e.,

$$\mathbf{f}_\mathbf{r} = \lambda\,\mathbf{r}_\mathbf{0} \tag{42}$$

and the second term corresponds to the *static contact friction* force along the tangential direction (no slip), i.e.,

$$\mathbf{f}_\mathbf{t} = (-k\,\boldsymbol{\omega}_\mathbf{t}(t))^\times\,\mathbf{r}_\mathbf{0}\,/r^2_0 \tag{43}$$

For the magnitude of the force $\mathbf{f}_\mathbf{t}$ the following holds,

$$\|\mathbf{f}_\mathbf{t}\| = a_s\mu_s\|\mathbf{f}_\mathbf{r}\|,\quad 0<a_s\le1 \tag{44}$$

where μ_s is the static friction coefficient.

It can be shown that the desired normal contact force, expressed in frame {n}, is,

$${}^n\mathbf{f}_\mathbf{r} = \lambda\,{}^n\mathbf{r}_\mathbf{0} = \frac{\|k\,\mathbf{r}^\times_\mathbf{0}\,\hat{\mathbf{k}}_\mathbf{t}\|\boldsymbol{\omega}_\mathbf{t}(0)\|\|}{a_s\mu_s\,r^2_0}\frac{\|\boldsymbol{\omega}_\mathbf{t}(t)\|}{\|\boldsymbol{\omega}_\mathbf{t}(0)\|}\,{}^n\hat{\mathbf{n}} = f^*_{d,e}\frac{\|\boldsymbol{\omega}_\mathbf{t}(t)\|}{\|\boldsymbol{\omega}_\mathbf{t}(0)\|}\,{}^n\hat{\mathbf{n}} \tag{45}$$

where $\boldsymbol{\omega}_t(0)$ is the initial target angular velocity and $\hat{\mathbf{k}}_t$ is the constant unit vector along the rotation axis.

Thus, the chaser's end-effector desired impedance behavior written in frame {n} is given again by (17), where the 6×1 desired force/ moment ${}^{n}\boldsymbol{F}_{\mathbf{d,e}}$ is given by (23) with,

$$ {}^{n}\boldsymbol{F}^{*}_{\mathbf{d,e}} = \| \boldsymbol{\omega}_t(t) \| / \| \boldsymbol{\omega}_t(0) \| \cdot f^{*}_{d,e} \cdot [\, 1,\ a_s \mu_s,\ \mathbf{0}_{1x4} \,]^T \qquad (46) $$

To avoid singular configurations and/ or end-effector slip, the chaser's S/C must be controlled. The chaser's S/C desired performance in inertial frame is given by (28); therefore, the system desired performance in inertial frame is governed by,

$$ \mathbf{M}_\mathbf{d}\,\ddot{\mathbf{e}} + \mathbf{B}_\mathbf{d}\,\dot{\mathbf{e}} + \mathbf{K}_\mathbf{d}\,\mathbf{e} = -\bar{\boldsymbol{F}}_{\mathbf{ext}} + \bar{\boldsymbol{F}}_\mathbf{d} \, \|\boldsymbol{\omega}_t\| / \|\boldsymbol{\omega}_t(0)\| \qquad (47) $$

where the external force/ moment $\bar{\boldsymbol{F}}_{\mathbf{ext}}$ is given by (34), the gains $\mathbf{M}_\mathbf{d}$, $\mathbf{B}_\mathbf{d}$, $\mathbf{K}_\mathbf{d}$ by (36) while $\bar{\boldsymbol{F}}_\mathbf{d}$ is given by (36), (22) and (23) - (24), with the desired force $f^{*}_{d,e}$ given by (45).

Considering (47) and (35), the system accelerations are

$$ \ddot{\mathbf{x}} = \mathbf{M}_\mathbf{d}^{-1} [-(\mathbf{B}_\mathbf{d}\,\dot{\mathbf{e}} + \mathbf{K}_\mathbf{d}\,\mathbf{e}) - \bar{\boldsymbol{F}}_{\mathbf{ext}} + \bar{\boldsymbol{F}}_\mathbf{d} \, \|\boldsymbol{\omega}_t\| / \|\boldsymbol{\omega}_t(0)\|] + \ddot{\mathbf{x}}_\mathbf{d} \qquad (48) $$

The combination of (16) and (48) results in the following coordinated control law

$$ \begin{aligned} &\mathbf{Q}_{\mathbf{act}} = \mathbf{Q}_{\mathbf{ext}} + \mathbf{c} + (\mathbf{J}\,\mathbf{H}^{-1})^{-1} \cdot \\ &\cdot [\ddot{\mathbf{x}}_\mathbf{d} + \mathbf{M}_\mathbf{d}^{-1}(-\bar{\boldsymbol{F}}_{\mathbf{ext}} + \bar{\boldsymbol{F}}_\mathbf{d} \, \|\boldsymbol{\omega}_t\| / \|\boldsymbol{\omega}_t(0)\| - \mathbf{B}_\mathbf{d}\,\dot{\mathbf{e}} - \mathbf{K}_\mathbf{d}\,\mathbf{e}) - \dot{\mathbf{J}}\,\dot{\mathbf{z}}] \end{aligned} \qquad (49) $$

and the actuator inputs computed using (39).

During the contact phase, the application of the control law de-spines the target to a steady state, i.e., $\boldsymbol{\omega}_t^{\mathbf{ss}} = \mathbf{0}_{3\times1}$; then, the end-effector can be detached from the target. The application of the developed control law (49), results in a desired end-effector performance, designated by (47), and affects the target motion, described by (2).

It is assumed that the contact force/ moment can be modeled as a spring force/ moment given by (18), and (22). The combination of equations (2) and (47) results in a nonlinear system of the form,

$$ \dot{\mathbf{y}} = \mathbf{g}(\mathbf{y}) \qquad (50) $$

where

$$ \mathbf{y} = [\mathbf{e}_{\mathbf{e,c}}^T \quad \dot{\mathbf{e}}_{\mathbf{e,c}}^T \quad \boldsymbol{\omega}_\mathbf{t}^T]^T \qquad (51) $$

$$ \mathbf{g}(\mathbf{y}) = \begin{bmatrix} \dot{\mathbf{e}}_{\mathbf{e,c}} \\ \mathbf{M}_{\mathbf{d,e}}^{-1}(-\mathbf{B}_{\mathbf{d,e}}\,\dot{\mathbf{e}}_{\mathbf{e,c}} - (\mathbf{K}_{\mathbf{d,e}} + \mathbf{K}_\mathbf{e})\mathbf{e}_{\mathbf{e,c}} + \bar{\boldsymbol{F}}_\mathbf{d} \|\boldsymbol{\omega}_t\| / \|\boldsymbol{\omega}_t(0)\|) \\ \mathbf{I}_\mathbf{t}^{-1}(\mathbf{r}_\mathbf{0}^{\times}\,\mathbf{K}_\mathbf{e}\,\mathbf{e}_{\mathbf{e,c}} - \boldsymbol{\omega}_\mathbf{t}^{\times}(\mathbf{I}_\mathbf{t}\,\boldsymbol{\omega}_\mathbf{t})) \end{bmatrix} \qquad (52) $$

For this system, the point

$$ \mathbf{y}^{*} = [\mathbf{e}_{\mathbf{e,c}}^{*T} \quad \dot{\mathbf{e}}_{\mathbf{e,c}}^{*T} \quad \boldsymbol{\omega}_\mathbf{t}^{*T}]^T = [\mathbf{0}_{\mathbf{6\times1}}^T \quad \mathbf{0}_{\mathbf{6\times1}}^T \quad \mathbf{0}_{\mathbf{3\times1}}^T]^T \qquad (53) $$

is an equilibrium, since,

$$ \dot{\mathbf{y}}^{*} = \mathbf{g}(\mathbf{y}^{*}) = \mathbf{0}_{\mathbf{15\times1}} \qquad (54) $$

Therefore, to achieve at the steady state $\boldsymbol{\omega}_\mathbf{t}^{\mathbf{ss}} = \mathbf{0}_{\mathbf{3\times1}}$ and $\mathbf{e}_{\mathbf{e,c}}^{\mathbf{ss}} = \mathbf{0}_{\mathbf{6\times1}}$, one must show that this equilibrium point is stable. Linearizing the non-linear system described by (50) around this equilibrium point, a linear system is obtained as,

$$ \dot{\mathbf{y}} = \mathbf{A}\,\mathbf{y} \qquad (55) $$

where the matrix $\mathbf{A}$ is given by,

$$ \mathbf{A} = \partial \mathbf{g} / \partial \mathbf{y} \big|_{\mathbf{y}=\mathbf{y}^{*}} \qquad (56) $$

Stability of the equilibrium point $\mathbf{y}^{*}$ requires selection of appropriate impedance gain matrices $\mathbf{M}_{\mathbf{d,e}}$, $\mathbf{B}_{\mathbf{d,e}}$, $\mathbf{K}_{\mathbf{d,e}}$ and $\boldsymbol{F}^{*}_{\mathbf{d.e}}$ so that $\mathbf{A}$ has left half plane eigenvalues.

V. EXAMPLES

To illustrate the proposed control laws, a planar chaser with a 3 DoF manipulator is employed, see Fig. 3. The chaser parameters are shown in Table I.

Table I. Parameters of the planar chaser shown in Fig. 3.

Body	l_i (m)	r_i (m)	m_i (Kg)	I_i(Kg m^2)
0	-	1.0	400	200
1	1.0	1.0	50	16.67
2	1.0	1.0	50	16.67
3	0.5	0.25	20	4.17

The target mass and moment of inertia are $m_t = 100\,Kg$ and $I_t = 50\,Kg\,m^2$, respectively. The contact between the two bodies is modeled by a spring of stiffness $k_e = 10\,kN/m$.

Example 1 – Target de-orbiting: The target is initially at rest at $(x_{t,in} \quad y_{t,in}) = (2.5 \quad 2.5)\ m$. The chaser's end-effector is driven to the target from an initial position $(x_{e,in} \quad y_{e,in}) = (6 \quad 7)\,m$ at $t = 100\,s$. The initial position of the S/C CoM is $(x_{b,in} \quad y_{b,in}) = (2.5 \quad 5)\,m$. The control law (38) is applied on the chaser both during the free-space and the contact phases. The desired distance between the end-effector and the chaser S/C is chosen as $\mathbf{s_0} = [2 \quad 2.5\ ]^T (m)$. The desired response of the end-effector mass in the free-space phase is defined by a damping ratio $\zeta_f = 1$ and a settling time $t_s = 10\,s$. To avoid loss of contact, the initial end-effector velocity during the contact is computed by (27).

The 6×6 diagonal matrices $\mathbf{M}_\mathbf{d}$, $\mathbf{B}_\mathbf{d}$ and $\mathbf{K}_\mathbf{d}$, and the 6×1 column vector $\bar{\mathbf{f}}_\mathbf{d}$ used in the control law (38) are

$$ \begin{aligned} &\mathbf{M}_\mathbf{d} = diag(277.8)\ , \quad \mathbf{B}_\mathbf{d} = diag(333.3)\ , \\ &\mathbf{K}_\mathbf{d} = diag(100), \qquad \bar{\boldsymbol{F}}_\mathbf{d} = [0.1 \quad \mathbf{0}_{\mathbf{1\times5}}]^T \end{aligned} \qquad (57) $$

The relative distance between the chaser's end-effector and S/C and the contact force are shown in Fig. 4(a). As can be seen, the desired distance between the S/C and the end-effector is achieved during the free space phase. The chaser does not lose contact with the target since the external force shown in Fig. 4(a) is always positive. The required forces/moments applied on the chaser's S/C by thrusters and reaction wheels as well as the joint torques, computed using (39) and displayed in Fig. 4(b) and Fig. 4(c), respectively, are small and smooth, guaranteeing the feasibility of the task.

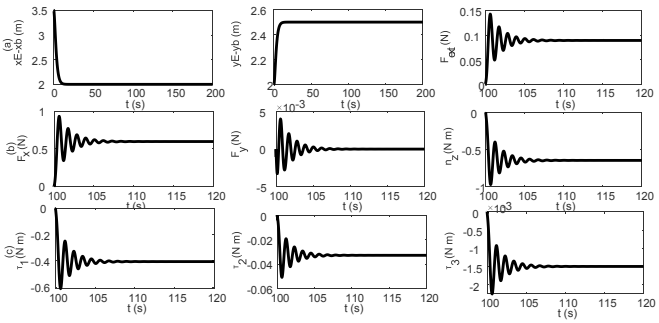

Fig. 4. (a) The relative position between the chaser's end-effector and S/C, and the contact force, (b) the applied force/ moment on the chaser S/C and (c) the applied joint torques during contact.

Example 2 – Target de-spinning: In the case of planar systems, (2) and (47) describing the de-spinning task, are linear and can be written directly in the form of (55). The system stability can be guaranteed by selecting the appropriate gains $m_{d,e}$, $b_{d,e}$, $k_{d,e}$ and $f_{d,e}^{*}$. The characteristic polynomial of the system, in this case, is,

$$p(s)=s^3+\frac{b_{d,e}}{m_{d,e}}s^2+\frac{k_{d,e}+k_e}{m_{d,e}}s+\frac{f_{d,e}^{*}\,k_e\,r_0}{I_t\,m_{d,e}\,\omega_t(0)} \tag{58}$$

where I_t is the target polar inertia and the contact is modelled as a spring of constant k_e. Therefore, the target de-spinning is expressed by third order dynamics and one can select the desired characteristic polynomial as,

$$p_d(s)=(s+a_c\zeta_c\omega_{n,c})(s^2+2\zeta_c\omega_{n,c}s+\omega_{n,c}^2) \tag{59}$$

where $\zeta_c>0$ and a_c a positive constant defines the desired location of the closed-loop system's third pole.

Then, the appropriate gains are selected as,

$$b_{d,e}=\zeta_c\omega_{n,c}(2+a_c)m_{d,e} \tag{60}$$

$$k_{d,e}=(1+2a_c\zeta_c^2)\omega_{n,c}^2\,m_{d,e}-k_e \tag{61}$$

$$f_{d,e}^{*}=a_c\zeta_c\omega_{n,c}^3\,I_t\,m_{d,e}\;\omega_t(0)\big/(k_e\,r_0) \tag{62}$$

Note, that it must be $k_{d,e}>0$; thus (61) yields,

$$m_{d,e}>k_e\big/((1+2a_c\zeta_c^2)\,\omega_{n,c}^2) \tag{63}$$

Therefore, to design the control law, first the gain $m_{d,e}$ is selected according to (63), and then the gains $b_{d,e}, k_{d,e}, f_{d,e}^{*}$ are computed using (60) - (62).

The continuous contact of the chaser end-effector with the target is guaranteed if $e_{e,c}(t)>0$ at the contact phase. Considering a desired critical damping response at the contact phase (i.e., $\zeta_c=1$), the response of the error $e_{e,c}$ is,

$$\begin{aligned}e_{e,c}(t)=&\frac{1}{1-a_c}\left(e^{-\omega_{n,c}t}\,t+\frac{e^{-\omega_{n,c}t}-e^{-a_c\omega_{n,c}t}}{\omega_{n,c}(1-a_c)}\right)\left(v_0-\frac{f_{d,e}^{*}}{m_d\,\omega_{n,c}}\right)\\&+\frac{e^{-\omega_{n,c}t}-e^{-a_c\omega_{n,c}t}}{\omega_{n,c}(a_c-1)}v_0\end{aligned} \tag{64}$$

where v_0 is the initial relative velocity of the chaser's end-effector along the contact direction with respect to the target.

It can be shown that $e_{e,c}(t)>0$ is satisfied in this case only if the relative velocity v_0 of the end-effector with respect to the target at the beginning of the contact ranges in,

$$0<v_0<f_{d,e}^{*}\big/(m_{d,e}\,\omega_{n,c}) \tag{65}$$

The required end-effector velocity $\dot{x}_{\mathbf{e}}(0)=v_o+\dot{x}_t(0)$ at the beginning of the contact phase is also the final end-effector velocity in the free-space phase and can be achieved by proper design of the desired trajectory $\mathbf{x}_{\mathbf{d,e}}^{\mathbf{f}}(t)$.

In summary, to de-spin the planar target in Fig. 3 with initial angular velocity $\omega_t(0)=0.5 rad/s$ by applying the control law (49), one selects the control gains (60) - (63), considering the desired end-effector performance during contact (e.g. $a_c=10$, $\zeta_c=1$ and $t_s=50\,s$).

Fig. 5(a) shows the target angular velocity during contact. As can be seen, target de-spinning is achieved in the desired time; following target de-spinning the end-effector stops exerting a contact force on the target, see Fig. 5(b).

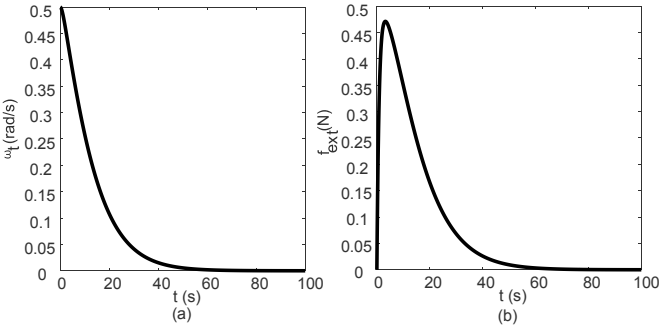

Fig. 5. (a) The target angular velocity during the contact phase and (b) the resulting contact force.

VI. Conclusion

In this paper, a coordinated impedance control law was developed to de-orbit a target via continuous contact between the chaser end-effector and the target. Since both the end-effector and the S/C are controlled, the controller guarantees singularity avoidance in addition to continuous contact between the two bodies. Next, this controller was modified to be applied in the de-spinning of a rotating satellite of known angular velocity via continuous contact. The proposed control laws are developed for spatial systems and were illustrated by planar examples.

References

[1] Lu, Y., Liu, X.G., Zhou, Y., and Liu, C.C., "Review of Detumbling Technologies for Active Removal of Uncooperative Targets," *Acta Astronautica*, 39, 2018, pp. 1 – 13.

[2] Schneider, S.A., Cannon Jr., R.H., "Object impedance control for cooperative manipulation: theory and experimental results," *IEEE Trans. Robotics Automation*, Vol. 8, No.3, 1992, pp. 383 - 394.

[3] Hirano, D., Kato, H., and Saito, T., "Online Path Planning and Compliance Control of Space Robot for Capturing Tumbling Large Object," *IEEE/RSJ International Conference on Intelligent Robots and Systems*, Madrid, Spain, Oct. 1-5, 2018, pp. 2909 - 2916.

[4] Sharma, S., Suomalainen, M., and Kyrki, V., "Compliant Manipulation of Free-Floating Objects," *IEEE Int. Conf. on Robotics and Automation,* May 21-25, Brisbane, QLD, Australia, 2018, pp. 865 - 872.

[5] Giordano, A. M., Calzolari, D., De Stefano, M., Mishra, H., Ott, C., Albu-Schaffer, A., "Compliant Floating-Base Control of Space Robots," *IEEE Robotics and Automation Letters*, 2021, pp. 7485 – 7492.

[6] Gangapersaud, R.A., Liu, G., de Ruiter, A.H.J., "Detumbling of a Non-cooperative Target with Unknown Inertial Parameters Using a Space Robot," *Advances Space Research*, 63, 2019, pp. 3900 – 3915.

[7] Wu, S., Mou, F., Liu, Q., Cheng, J., "Contact Dynamics and Control of a Space Robot Capturing a Tumbling Object," *Acta Astronautica*, 151, 2018, pp. 532 – 542.

[8] Zang, Y., Zhang, Y., Zhang, J., Guo, Z., Chen, Y., and Chen, S., "Multipoint contact dynamics and the detumbling strategy for a fast-tumbling target," *IEEE Transactions on Aerospace and Electronic Systems*, 56 (4), 2019, pp. 3113 – 3122.

[9] Wang, M., Luo, J., Yuan, J., and Walter, U., "An Integrated Control Scheme for Space Robot After Capturing Non-cooperative Target," *Acta Astronautica*, 147, 2018, pp. 350 – 363.

[10] Shi, L., Xiao, X., Shan, M., and Wang, X., "Force Control of a Space Robot in On-orbit Servicing Operations," *Acta Astronautica*, 193, 2022, pp. 469 – 482.

[11] Nanos, K., Xydi-Chrysafi, F., and Papadopoulos, E., "On Impact Deorbiting for Satellites Using a Prescribed Impedance Behavior," *IEEE 58th Conference on Decision and Control,* Nice, France, Dec. 11-13, 2019, pp. 2126 – 2131.